ANALYSIS OF STATIC AND DYNAMIC HORIZONTAL LOAD TESTS ON STEEL PIPE PILES

Pastsakorn Kitiyodom, Kanazawa University, Kanazawa, Japan

Tatsunori Matsumoto, Kanazawa University, Kanazawa, Japan

Eiji Kojima, Japan Pile Corporation, Tokyo, Japan

Hiromichi Kumagai, Japan Pile Corporation, Tokyo, Japan

Kouichi Tomisawa, Civil Engineering Research Institute of Hokkaido, Hokkaido, Japan

In order to estimate the deformation and load distribution of a single pile subjected to dynamic horizontal load as well as vertical load, a simplified method of three-dimensional numerical analysis, KWaveHybrid program, is developed using a hybrid model. In the hybrid model, the pile is modelled as elastic beams, and the soil at each pile node is treated as springs and dashpots in both vertical and horizontal directions. KWaveHybrid is also able to analyse the static response of the pile. Validity of the newly developed program is examined through comparisons with theoretical values and horizontal dynamic and static pile load test results

INTRODUCTION

It has been believed that the static load test is the most reliable method to obtain the load-displacement relation of a pile. Most static load tests are conducted using reaction piles as the reaction system. In the work of Kitiyodom et al. (2004), it is suggested that the influence of the reaction piles on the measured load-displacement relation may not be neglected, and that an interpretation of the measured data is required to obtain a true load-displacement relation of the pile.

For axial compressive pile load test, the dynamic load testing or the rapid load testing is widely used because of the fact that these methods are unsusceptible to reaction piles, and require less time and cost compared with the conventional static load test where reaction piles are employed. The dynamic load testing and the rapid load testing, however, require interpretation of the measured signals to derive a corresponding static load-displacement relation. Especially, for dynamic load test in which wave propagation phenomena in the pile cannot be neglected, wave matching analysis is indispensable.

In a seismic area such as Japan, application of the dynamic or rapid pile load test to horizontal pile load testing would be very useful in the seismic design of the pile foundation. Several computer programs for analysing the one-dimensional wave propagation in a pile have been developed, such as Smith method (Smith, 1960), CAPWAP (Rausche et al., 1972), WEAP (Goble & Raushe, 1976), TNOWAVE (TNO, 1977), KWave (Matsumoto & Takei, 1991) and KWaveFD (Wakisaka et al., 2004). However, all of these programs can be applied to the problem in vertical direction only.

In this study, a computer program KWaveHybrid has been developed based on a hybrid model. In KWaveHybrid, the horizontal resistance of the piles is incorporated into the hybrid model so as to be able to analyse the deformation and load distribution of a single pile subjected to horizontal load as well as vertical load. The program can be also used to calculate the static load-displacement relation of the pile in both horizontal and vertical directions.

In order to examine the validity of the newly developed program, verification analyses are carried out first. Then the program is applied to

the static and dynamic horizontal load tests of actual steel pipe piles.

METHOD OF ANALYSIS

Fig. 1 illustrates the hybrid modelling of the pile and the soil used in this study. The pile is modelled as beam elements with masses and the soil is treated as springs and dashpots.

Fig. 2 shows the dynamic shaft soil resistance model incorporated into KWaveHybrid. The values of the vertical spring, k, the horizontal springs, k^x and k^y, the vertical radiation damping, c, and the horizontal radiation damping, c^x and c^y, per unit shaft area are approximated by means of Eqs. 1 and 2, based on the work of Novak et al. (1978).

$$k = \frac{2.75G_s}{\pi d},\ k^x = k^y = \frac{4G_s}{d} \tag{1}$$

$$c = \frac{G_s}{V_s},\ c^x = c^y = \frac{4.5G_s}{V_s} \tag{2}$$

where G_s and V_s are the shear modulus and the shear wave velocity of the surrounding soil respectively, and d is the outer diameter of the pile.

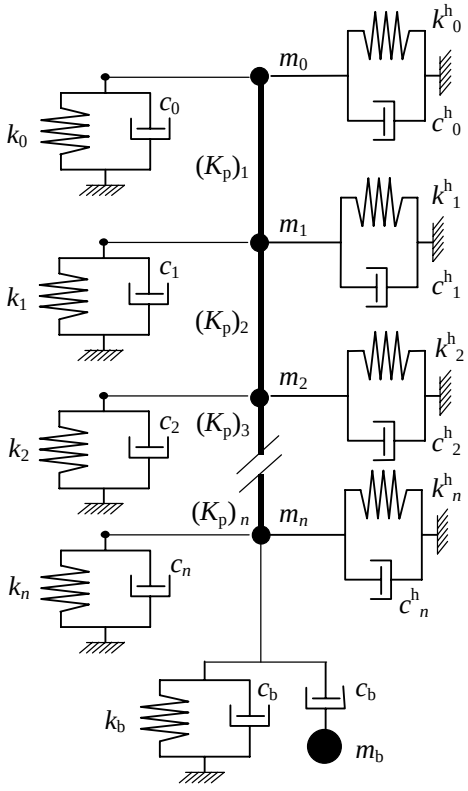

Fig. 1. Hybrid modelling of the pile and the soil.

The slider value is equal to the static maximum shaft resistance in the vertical direction and is equal to the limit horizontal pressure in the horizontal direction.

The total dynamic friction in vertical direction, τ_{total}, is generally taken as a non-linear function of velocity, according to

$$\tau_{total} = \tau_{static}^{max}\left[1+\alpha\left(\Delta v / v_0\right)^{\beta}\right] \quad (v_0 = 1\ \text{m/s}) \tag{3}$$

where v_0 is a reference velocity and Δv is the relative velocity between the pile and the adjacent soil. Non-linear viscous laws similar to Eq. 3 have been proposed by Gibson & Coyle (1968), Heerema (1979), and Litkouhi & Poskitt (1980), all of whom suggest a value of β close to 0.2, with the parameter α varying from about 0.1 for sand, to unity for clay soils (Randolph & Deek, 1992). The relation in Eq. 3 was introduced into the viscous damping in Fig. 2 for vertical shaft resistance model.

Fig. 3 shows the dynamic vertical pile base resistance model. The values of the soil spring at the pile base, k_b, the damping, c_b, and the lumped soil mass, m_b, per unit base area can be estimated as follows (Deek & Randolph, 1995):

$$k_b = \frac{8G_s}{\pi d(1-\nu_s)} \tag{4}$$

$$c_b = \frac{3.4}{\pi(1-\nu_s)}\frac{G_s}{V_s} \tag{5}$$

$$m_b = 16 r_o \rho_s \frac{0.1-\nu_s^4}{\pi(1-\nu_s)} \tag{6}$$

in which ν_s and ρ_s are the Poisson's ratio and the density of the soil respectively.

The equation of motion of the pile is expressed as

$$[K]\{w\} + [C]\{\dot{w}\} + [M]\{\ddot{w}\} = \{F\} \tag{7}$$

where [K], [C] and [M] are the stiffness matrix, the damping matrix and the mass matrix respectively. {F} is the external force vector. The stiffness matrix is formed from the pile stiffness matrix and the soil stiffness matrix. The damping matrix is equal to the soil damping matrix. The mass matrix is formed from the pile mass matrix and the lumped soil mass at the pile base.

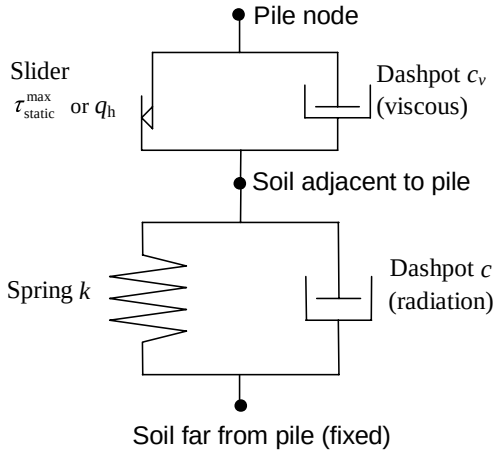

Fig. 2. Vertical and horizontal shaft resistance model.

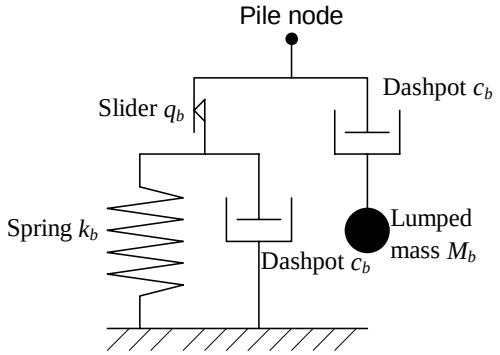

Fig. 3. Vertical base resistance model.

When the stress at a pile-soil interface nodal point reaches the soil yield stress, the soil spring stiffness and the dashpot value at that point are set to 0. In order to consider also the nonlinearity of the soil spring stiffness, Eq. 7 is rewritten in incremental form as:

$$\{F\}_t + [K]_t \{\Delta w\}_{t+\Delta t} + [C]_t \{\dot{w}\}_{t+\Delta t} + [M]_t \{\ddot{w}\}_{t+\Delta t} = \{F\}_{t+\Delta t} \quad (8)$$

Eq. 8 can be solved for the pile settlements, deflections and rotations from which the axial forces, the shear forces and the bending moments can be obtained. Note that Newmark's β method (NewMark, 1959) is used for solving Eq. 8.

In the analysis of static pile load test, the static vertical shaft soil spring, k_{static}, is estimated by means of Eqs. 9 and 10 following Randolph and Wroth (1978).

$$k_{static} = (2\pi / 2.75\xi) \cdot k \,,\ \xi = \ln[5.0(1-\nu_s)l / d] \quad (9)$$

where l is the pile embedment length.

The static horizontal shaft soil spring values at each pile node are estimated based on Mindlin's solution (Mindlin, 1936) which is similar to the solution of the integral equation method used by Poulos and Davis (1980). The equations become

$$k^x_{static} = k^y_{static} = \zeta E_s \Delta l \quad (10)$$

$$\zeta = pd / uE_s \quad (11)$$

where p is the horizontal distributed force acting uniformly over the pile element and u is the corresponding horizontal displacement at each pile node calculated using the integral equation method.

Note that the shear resistance at the pile base has not been incorporated in the present program. More details of the static analysis method can be found in Kitiyodom & Matsumoto (2002, 2003).

ACCURACY OF THE PROPOSED METHOD

Impacts on pile without soil resistance

Vertical impacts on a homogeneous pile and a non-homogeneous pile without soil resistance are calculated by the program KWaveHybrid, and the calculated results are compared with the theoretical values. Table 1 shows the specifications of a homogeneous pile to be analysed here.

Fig. 4 shows the vertical impact force applied to the pile head. Fig. 5 shows the calculated and theoretical distributions of axial forces along the pile. Theoretically, the front of compression force reaches the pile base at t = 2 ms because the bar wave velocity is 5000 m/s. The compression force is reflected at the pile base, and the reflected force goes back to the pile head as the tension force and reaches the pile head at t = 4 ms. The calculated results are in good agreements with these theoretical solutions. Fig. 6 shows the time vs pile displacement at the middle point (z = 5 m). A good agreement between the theoretical and calculated values can be seen again.

Table 1. Specifications of a homogeneous pile.

Length (m)	10
Diameter (mm)	400
Cross-sectional area (m^2)	0.126
Young's modulus (kN/m^2)	3.0×10^7
Bar wave velocity (m/s)	5000
Density (ton/m^3)	1.2
Mass (ton)	1.51

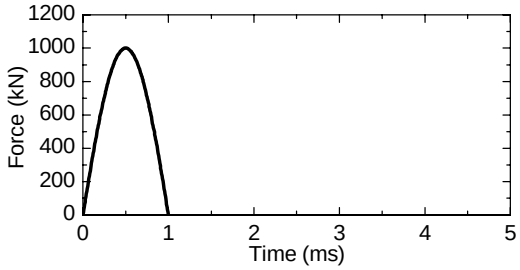

Fig. 4. Pile head force.

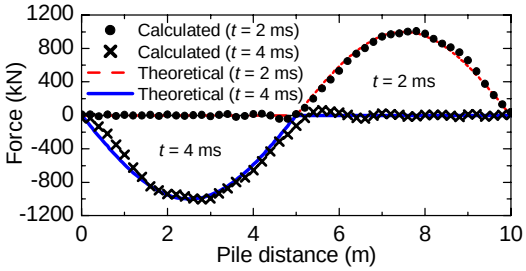

Fig. 5. Distribution of axial force along the pile.

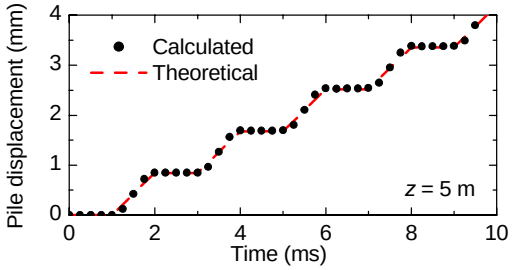

Fig. 6. Time vs pile displacement.

Table 2. Specifications of a non-homogeneous pile.

	Upper	Lower
Length (m)	5	5
Diameter (mm)	100	141.4
Cross section area (m^2)	7.85×10^{-3}	15.7×10^{-3}
Young's modulus (kN/m^2)	3.0×10^{7}	3.0×10^{7}
Bar wave velocity (m/s)	5000	5000
Density (ton/m^3)	1.2	1.2

A non-homogeneous pile with no soil resistance shown in Table 2 was also analysed using the proposed method. The pile consists of two sections having the same material but different cross-sectional areas. The cross-sectional area of the lower section is twice that of the upper section. The impact force shown in Fig. 4 was applied to the pile head.

Figs. 7 and 8 show time vs velocity and time vs pile head displacement, respectively. Good agreements between the calculated and theoretical values can be seen in both the velocity and displacement.

Friction pile with elastic soil response

A perfect friction pile with elastic friction response is analysed, and the calculated results are compared with the theoretical solutions of the single mass system shown in Fig. 9.

Specifications of the pile to be analysed here are the same as those shown in Table 1. The values of the vertical shaft spring stiffness, k, and the vertical radiation damping, c, were set as $k = 2.0\times10^3$ kN/m^3 and $c = 5.0$ kNs/m^3 along the pile shaft uniformly for convenience. The corresponding values of the total vertical spring stiffness, K, and the total vertical damping, C, in the single mass system are shown in Fig. 9.

Figs. 10 and 11 show time vs displacement of the middle point of the pile without damping (c = 0) and with damping, respectively. Overall, the calculated results are in good agreement with the theoretical solutions in both cases. Periodical oscillations can be seen in the calculated results. These oscillations in the calculation results reflect the wave propagation phenomena in the pile, which cannot be simulated using the single mass system.

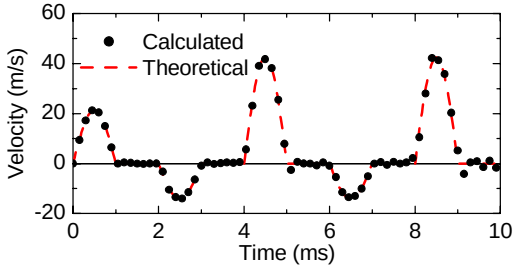

Fig. 7. Time vs pile head velocity.

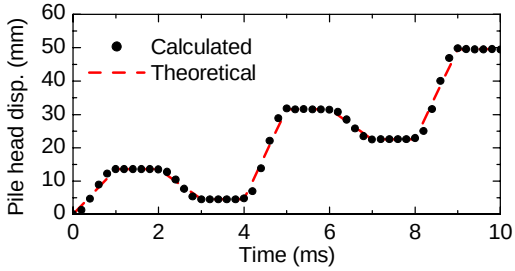

Fig. 8. Time vs pile head displacement.

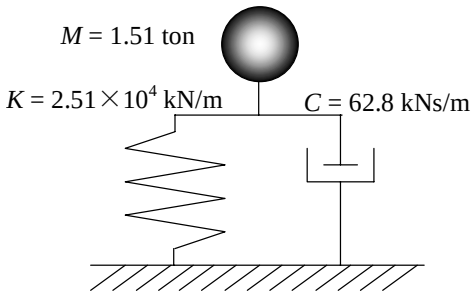

Fig. 9. Single mass system.

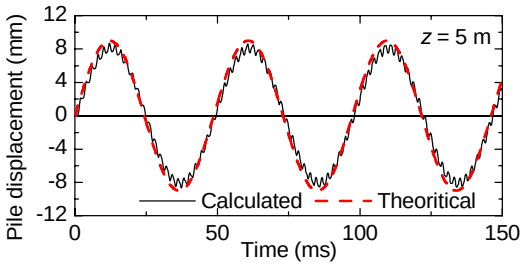

Fig. 10. Time vs pile displacement (without damping).

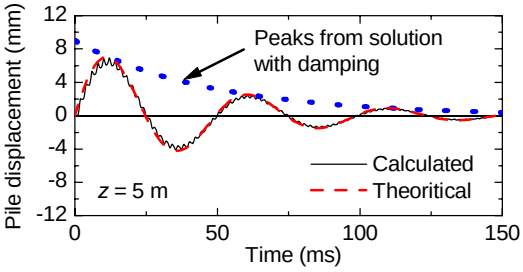

Fig. 11 Time vs pile displacement (with damping).

CASE STUDY

Test description

The test piling on two steel pipe piles was performed. Fig. 12 shows the profiles of soil layer and the SPT *N*-values at the test site. Two test piles, designated as P1 and P2, were installed by preboring. So there is no soil plug inside the piles. The test pile specifications are summarised in Table 3. The distance between the centres of the two piles is 3.5 m.

Both static and dynamic horizontal load tests were carried out on each pile. The dynamic pile load test was carried out prior to the static pile load tests. In the dynamic pile load test, the pile was hit horizontally by a hammer mass of 0.96 ton at the point z = 0.25 m below the pile head. Applied force, horizontal displacements and accelerations were measured at the same level of the hit point with a sampling rate of 15 ms.

After the dynamic pile load test, two static horizontal pile load tests with different loading methods were conducted on each pile. Static horizontal pile load test with step loading method (JSSMFE, 1983) was conducted first. Load step sequence for the step loading is shown in Fig. 13, following JSF T32-8320). In vertical pile load test standard JGS 1811-200221), two loading methods are recommended which are the step loading method and the continuous loading methods. However, in JSF T32-83, only the step loading method is prescribed. In this study, the static horizontal pile load test with the continuous loading method was also conducted. The load step sequence of continuous loading is also shown in Fig. 13. The static horizontal load was applied at the same loading point as the dynamic horizontal pile load test. The horizontal displacement of the pile and the applied force were monitored throughout the static pile load tests.

Table 3. Specifications of test steel piles

	P1	P2
Length (m)	6.5	10.0
Embedment length (m)	5.4	8.9
Outer diameter (mm)	600	500
Inner diameter (mm)	582	482
Cross-sectional area (cm^2)	167.1	138.8
Young's modulus (kN/m^2)	2.06×10^8	2.06×10^8
Shear wave velocity (m/s)	3187	3187
Density (ton/m^3)	7.8	7.8
Pile mass (ton)	0.9	1.1

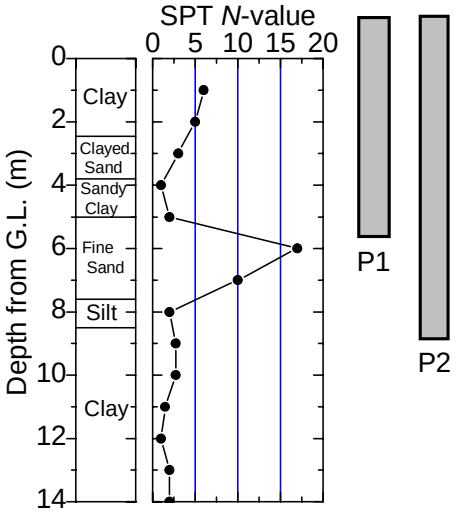

Fig. 12. Profiles of soil layers and SPT *N*-values.

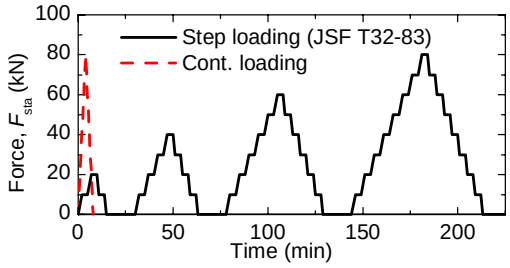

Fig. 13. Load step sequence of static pile load tests.

Measured static and dynamic test signals

The dynamic test signals of P1 and P2 are shown in Figs. 14 and 15, respectively. The measured forces increase and decrease rapidly with time and have a peak of about 50 kN. The loading duration is about 50 ms.

The measured static and dynamic horizontal load-horizontal displacement relations of P1 and P2 are shown in Figs. 16 and 17, respectively. It can be seen from the figures that there are good agreements between the measured load displacement relations from the static load tests with continuous loading and that from the static load tests with step loading. On the other hand, the measured load displacement relations from the dynamic load tests are totally different from the measured static load displacement relations. Therefore, in order to obtain the static load displacement relation of the pile from the measured signals of the dynamic load test, wave matching analysis of the measured dynamic signals was carried out using KWaveHybrid.

Wave matching analysis results

Matching analysis was repeated with assumed values for the maximum shaft limit horizontal pressure, q_h, and the soil shear modulus, G_s, using the measured F_{dyn} as the force boundary condition at the loading point, until a good matching between the calculated and the measured pile displacement was obtained. Soil parameters used in the final matching of P1 are listed in Table 4. Fig. 14(b) and Fig. 18 show the displacement vs time and load displacement relation of P1 in the final matching analysis, compared with the measured values.

It can be seen that the calculated dynamic pile displacement underestimated the measured values after the peak displacement. This is thought to be due to the soil spring model. At the present, the value of the soil springs in KWaveHybrid during the loading and unloading states are the same. It can be seen from the measured results (Figs. 16 and 17) that the values of the soil spring during the loading and unloading states should be different. These extensions are left for future work.

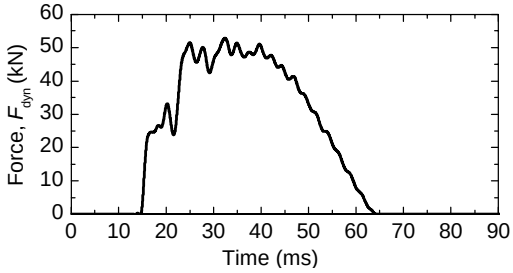

(a) Measured force

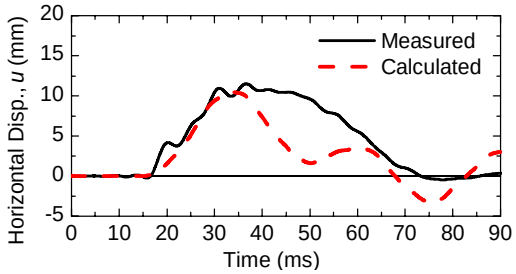

(b) Measured and estimated displacement

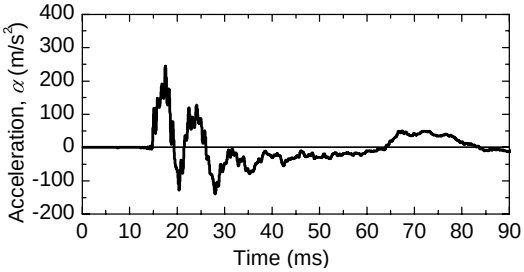

(c) Measured acceleration

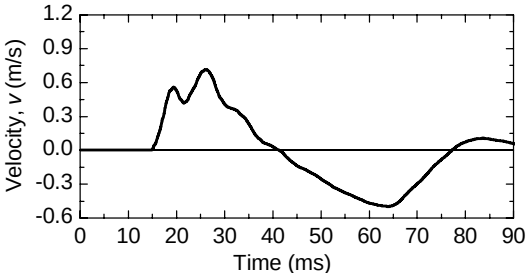

(d) Velocity (integrate of acceleration by time)

Fig. 14. Dynamic pile load test signals of P1.

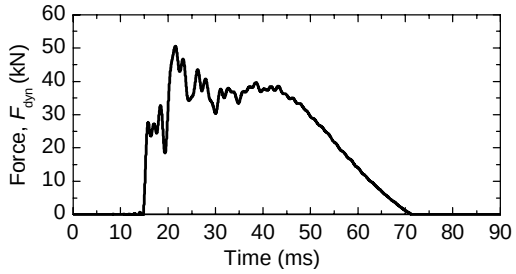

(a) Measured force

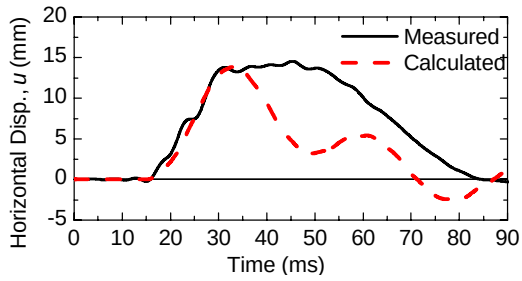

(b) Measured and estimated displacement

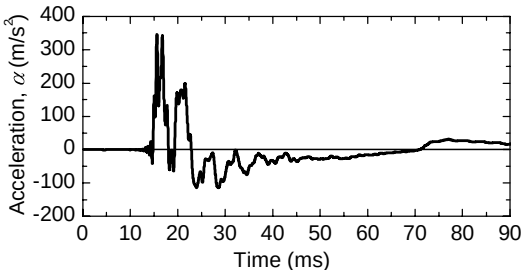

(c) Measured acceleration

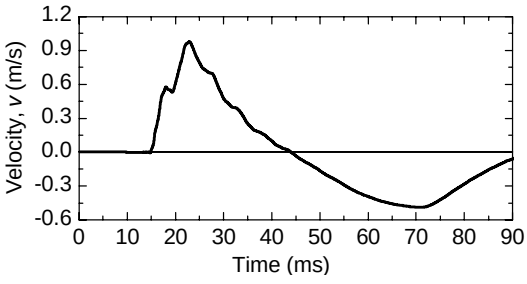

(d) Velocity (integrate of acceleration by time)

Fig. 15. Dynamic pile load test signals of P2.

Using the same soil parameters as shown in Table 4, the static load displacement relation of P1 was estimated using KWaveHybrid. Fig. 19 shows the comparison of the estimated static load displacement relation of P1 with the measured value. It can be seen that the estimated result matches very well with the measured one.

The same analysis procedures as P1 were carried out for P2. Soil parameters used in the final matching of P2 are listed in Table 5. Fig. 15(b) and Fig. 20 show the displacement vs time and load displacement of P2 in the final matching analysis, compared with the measured values.

Fig. 21 shows the comparison of the estimated static load displacement relation of P2 with the measured value. Again there is a good agreement between the estimated and the measured results.

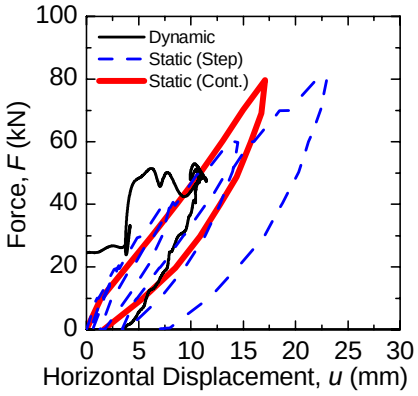

Fig. 16. Measured load-displacement of P1

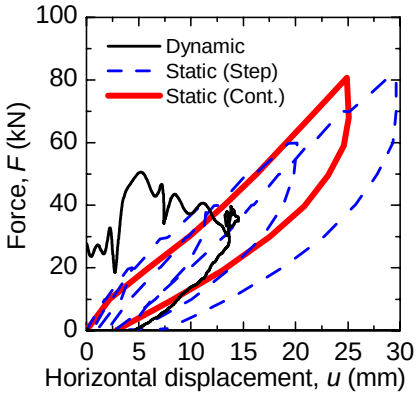

Fig. 17. Measured load-displacement of P2

Table 4. Parameters for final matching of P1.

Depth (m)	G_s (kPa)	ν_s	q_h (kPa)
0 to 1	1083	0.3	1
> 1	1083	0.3	Elastic range

Table 5. Parameters for final matching of P2.

Depth (m)	G_s (kPa)	ν_s	q_h (kPa)
0 to 1	1539	0.3	5
> 1	1539	0.3	Elastic range

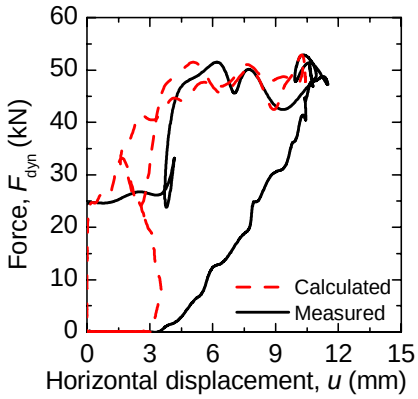

Fig. 18. Dynamic pile load test results of P1

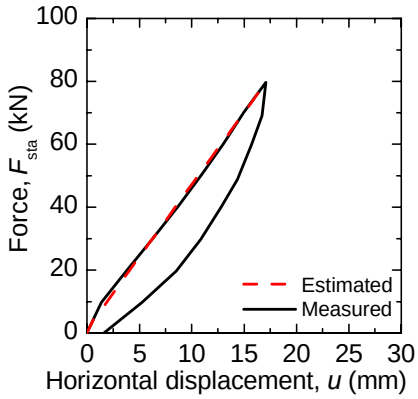

Fig. 19. Static pile load test results of P1.

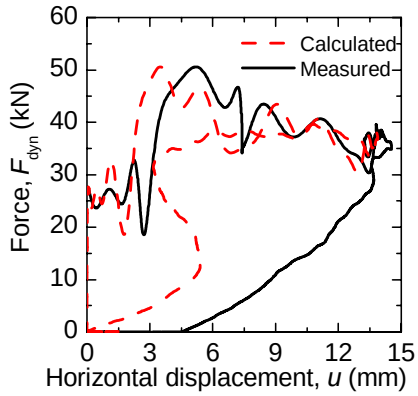

Fig. 20. Dynamic pile load test results of P2.

Prediction analysis

In actual construction site, it would be very useful to estimate the static load displacement relation of the actual pile from the dynamic load test of another pile having smaller diameter. In this work, the soil parameters of P2 (Table 5), which has a smaller diameter than P1, were employed to predict the load displacement relation of P1.

Fig. 22 shows the predicted displacement vs time and the predicted dynamic load displacement relation of P1, compared with the measured values.

Fig. 23 shows the predicted static load displacement relation of P1, compared with the measurement. It can be seen from the figures that although the predicted displacements overestimate the measured values, there are reasonable agreements between the predicted and the measured values.

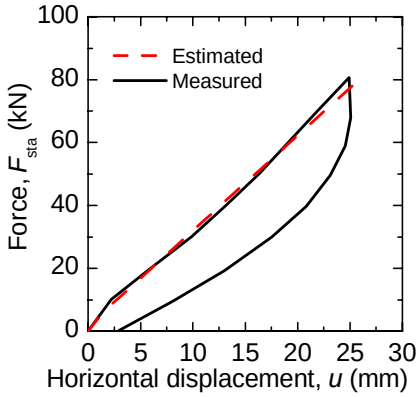

Fig. 21. Static pile load test results of P1.

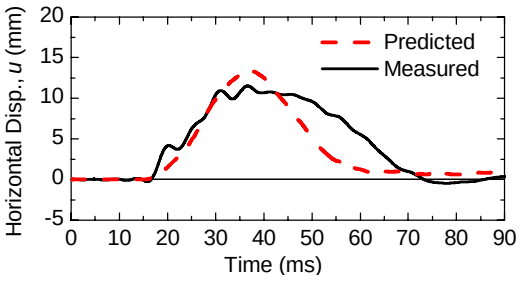

(a) Measured and predicted displacement.

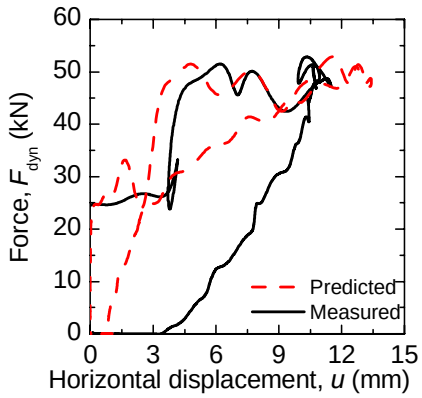

(b) Measured and predicted load-displacement.

Fig. 22. Predicted dynamic results of P1.

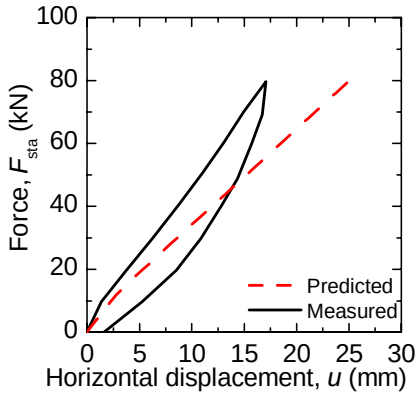

Fig. 23. Predicted static load-displacement of P1.

CONCLUSIONS

A new numerical program KWaveHybrid for analysing pile driving as well as static load test in vertical and horizontal directions has been developed in this study. Performance of the program was verified through comparisons with theoretical solutions

The developed program was then applied to the dynamic and static horizontal load tests on two steel pipe piles. A good matching between the calculated and measured behaviours of the piles during driving and during static load test was obtained.

The identified soil resistance parameters of the smaller diameter pile were used to predict the behaviours of the bigger pile, and a good prediction was obtained.

REFERENCES

Deek, A. J. and Randolph, M. F., 1995. A simple model for inelastic footing response to transient loading. *International Journal for Numerical and Analytical Methods in Geomechanics*, 19, 307-329.

Gibson, G. and Coyle, H. M., 1968. Soil damping constant related to common soil properties in sands and clays. Report No. 125-1, Texas Transport Institute, Texas A&M University.

Goble, G. G. and Rausche, F., 1976. Wave equation analysis of pile driving-WEAP program, prepared for the U.S. department of transportation, federal highway administration, implementation division, office of research and development.

Heerema, E. P., 1979. Relationships between wall friction displacement, velocity and horizontal stress in clay and in sand for pile driveability analysis. Ground Engineering, 12(1).

Japanese Geotechnical Society, 2002. *Standards of Japanese Geotechnical Society for vertical load tests of piles*. Japanese Geotechnical Society, Tokyo.

Japanese Society of Soil Mechanics and Foundation Engineering, 1983. *JSSMFE standard method for lateral loading test for a pile*. Japanese Society of Soil Mechanics and Foundation Engineering, Tokyo.

Kitiyodom, P. and Matsumoto, T., 2002. A simplified analysis method for piled raft and pile group foundations with batter piles. *International Journal for Numerical and Analytical Methods in Geomechanics*, 26, 1349-1369.

Kitiyodom, P. and Matsumoto, T., 2003. A simplified analysis method for piled raft foundations in non-homogeneous soils. *International Journal for Numerical and Analytical Methods in Geomechanics*, 27, 85-109.

Kitiyodom, P., Matsumoto, T. and Kanefusa, N., 2004. Influence of reaction piles on the behaviour of test pile in static load testing. *Canadian Geotechnical Journal*, 41(3), 408-420.

Litkouhi, S. and Poskitt, T. J., 1980. Damping constant for pile driveability calculations. *Géotechnique*, 30(1), 77-86.

Matsumoto, T. and Takei, M., 1991. Effects of soil plug on behaviour of driven pipe piles. *Soil and Foundations*, 3(2), 14-34.

Mindlin, R. D., 1936. Force at a point interior of a semi-infinite solid. *Physics*, 7, 195-202.

Newmark, N. M., 1959. A method of computation for strucural dynamics. *Journal of the Engineering Mechanics Division ASCE*, 85(EM3), 67-94.

Novak, M., Nogami, T. and Aboul-Ella F., 1978. Dynamic soil reactions for plane strain case. *Journal of Mechanical Engineering ASCE*, 104(EM4), 953-959.

Poulos, H. G. and Davis E. H., 1980. *Pile Foundation Analysis and Design*, Wiley, New York.

Randolph, M. F. and Deeks A. J., 1992. Dynamic and static soil models for axial pile response. *Proceedings of the 4th International Conference on the Application of Stresswave Theory to Piles*, The Hague, 3-14.

Randolph, M. F. and Wroth, C. P., 1978. Analysis of deformation of vertically loaded piles. *Journal of Geotechnical Engineering ASCE*, 104(12), 1468-1488.

Rausche, F., Moses, F. and Goble, G. G., 1972. Soil resistance predictions from pile dynamics *Journal of the Soil Mechanics and Foundation Division ASCE*, 98(SM9), 917-937.

Smith, E. A. L., 1960. Pile driving analysis by the wave equation. *Journal of the Soil Mechanics and Foundation Division ASCE*, 86(SM4), 35-61.

TNO, 1977. Dynamic pile testing. Report No. BI-77-13.

Wakisaka, T., Matsumoto, T., Kojima, E. and Kuwayama S., 2004. Development of a new computer program for dynamic and static pile load tests. *Proceedings of the 7th International Conference on the Application of Stresswave Theory to Piles*, Kuala Lumpur, 341-350.